

A Temperature-Sensitive Liposomal ^1H CEST and ^{19}F Contrast Agent for MR Image-Guided Drug Delivery

Sander Langereis,^{*,†} Jochen Keupp,[‡] Juliën L. J. van Velthoven,[†] Inge H. C. de Roos,[†]
Dirk Burdinski,[†] Jeroen A. Pikkemaat,[†] and Holger Grull[†]

*Philips Research Europe, High Tech Campus 11, 5656 AE Eindhoven, The Netherlands, and
Philips Research Europe, Röntgenstrasse 24-26, 22335 Hamburg, Germany*

Received November 7, 2008; E-mail: sander.langereis@philips.com

Cancer therapy using systemically administrated cytostatic drugs typically causes severe side effects mainly due to an undesired biodistribution of low molecular weight drugs. A larger therapeutic window with less side effects of the treatment can be achieved by localized delivery of the cytostatics from a liposomal nanocarrier.¹ Liposomal drug therapy becomes particularly effective if the drug release is triggered by an external stimulus, for example localized hyperthermia induced by focused ultrasound.² Temperature-sensitive liposomes release encapsulated molecules near the melting temperature (T_m) of their lipid membrane as it transforms from a gel to a liquid crystalline phase. For instance, temperature-sensitive liposomes constructed from monopalmitoylphosphocholine (MPPC) and dipalmitoylphosphocholine (DPPC) have been used for the localized delivery of doxorubicin to tumors in response to a mild hyperthermic treatment (39–42 °C).³ Temperature-sensitive paramagnetic liposomes have also been explored as contrast agents for drug delivery guided by T_1 -weighted magnetic resonance imaging (MRI).⁴ In this approach, Gd(III) complexes are incorporated in the lumen of the liposome. Below T_m the MRI contrast agent remains within the liposome and the overall T_1 -relaxation enhancement is limited by the transmembrane water exchange rate, which results in a moderate contrast enhancement. Upon heating, the T_1 -based contrast enhancement goes through a maximum at T_m and subsequently decreases because of the release of the Gd(III) complex from the lumen of the liposome.⁴

An alternative method to generate contrast enhancement in MRI utilizes chemical exchange saturation transfer (CEST) hereby altering the signal of the bulk water via proton exchange processes.^{5–10} In a particularly sensitive class of CEST agents, lipoCEST agents, the rapid exchange of water molecules across phospholipid membranes is utilized to achieve chemical exchange of magnetically labeled water molecules.¹¹ Liposomes encapsulating a chemical shift agent provide a pool of water protons in their aqueous core that can be selectively saturated using a narrow radio frequency (RF) pulse, and subsequently the saturation is transferred to the not chemically shifted water of the bulk phase. The amount of magnetization transfer and, hence, the CEST contrast enhancement are determined by the transmembrane water diffusion rate, the amount of intraliposomal water, and the RF power used for selective saturation. More recently, Aime et al. demonstrated that the frequency of the intraliposomal water resonance peak can be shifted further away from the bulk water signal by deforming the lipid-vesicles into nonspherical liposomes upon dialysis under hypertonic conditions, which improves the frequency resolution.^{12,13}

Here, we report on a combined temperature-sensitive liposomal ^1H CEST and ^{19}F MR contrast agent as a potential carrier system

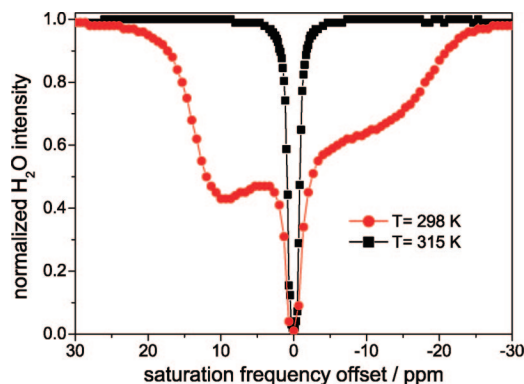


Figure 1. The Z-spectra ($B_1 = 4.5 \mu\text{T}$) of liposomes containing $[\text{Tm}(\text{hpdo3a})(\text{H}_2\text{O})]$ and NH_4PF_6 at 298 K (red dots) and 315 K (black squares) ($B_0 = 7 \text{ T}$).

for MRI guided drug delivery in combination with local hyperthermia induced by focused ultrasound. In their lumen, these liposomes contain both a chemical shift agent (for ^1H lipoCEST detection) as well as a highly fluorinated compound (for ^{19}F detection). Upon reaching the melting temperature of the agents' lipid membrane, the lipoCEST contrast enhancement vanishes, due to the release of the chemical shift agent. Simultaneously, the ^{19}F MRI probe is freed from the influence of the paramagnetic shift agent causing an appearance of a ^{19}F MRI signal. The combined CEST and ^{19}F MR temperature-sensitive liposomal carrier provides CEST-based contrast enhancement, which can be switched on and off at will, to localize the liposomes before release, while the ^{19}F MR signal can potentially be used to quantify the local release of drugs with MRI.

Temperature-sensitive liposomes (MPPC/DPPC/DPPE-PEG2000, 10:90:4) containing compartmentalized $[\text{Tm}(\text{hpdo3a})(\text{H}_2\text{O})]$ (65 mM) as a chemical shift agent^{13,14} and NH_4PF_6 (50 mM) as a ^{19}F MRI probe were prepared using the lipid film hydration technique working at 60 °C. The resulting dispersion was extruded successively through polycarbonate filters with pore sizes of 400, 200, and 100 nm. The obtained mainly unilamellar vesicles were dialyzed under hypertonic conditions to yield osmotically shrunken, non-spherical liposomes as evidenced from cryo-transmission electron microscopy (Figure S1). The Z-spectra of the liposomes containing the encapsulated chemical shift agent (Figure 1) and NMR spectra of the ^{19}F probe were recorded below and above the liposomal T_m of 311 K. At 298 K, the Z-spectrum showed direct saturation of the bulk water signal at a saturation frequency offset of 0 ppm and two signals at 11 and –17 ppm with CEST effects of 32% and 14%, respectively (Figure S2).

The CEST effect was calculated according to $\% \text{CEST} = (M_s - M_{\text{CEST}}) / M_s \times 100\%$, in which M_s is the magnitude of the bulk

[†] Philips Research Europe, The Netherlands.

[‡] Philips Research Europe, Germany.

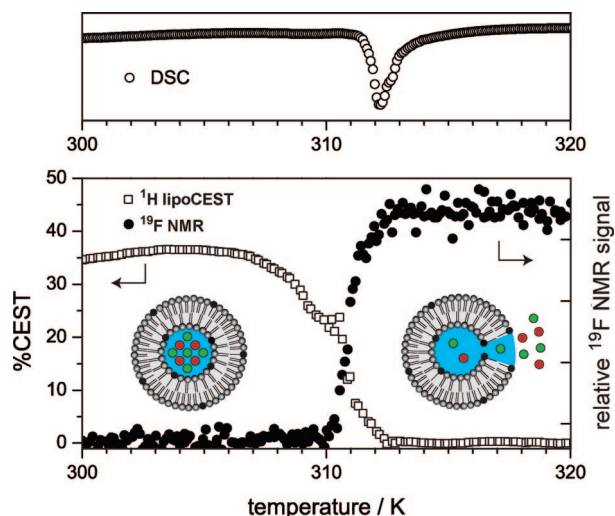


Figure 2. The ^1H CEST effect ($B_1 = 4.5 \mu\text{T}$) and the ^{19}F NMR signal intensity of liposomes containing $[\text{Tm}(\text{hpdo}3\text{a})(\text{H}_2\text{O})]$ and NH_4PF_6 as a function of temperature at $B_0 = 7 \text{ T}$ (lower panel). The DSC thermogram shows the melting temperature of the lipid membrane (upper panel).

water signal during saturation on resonance, and M_{-s} is the intensity of the bulk water signal at the opposite saturation frequency offset. The saturation frequency offset of the intraliposomal water at 11 ppm is in agreement with a literature report on nonspherical DPPC/DSPE-PEG2000-based liposomes containing entrapped $[\text{Tm}(\text{hpdo}3\text{a})(\text{H}_2\text{O})]$.¹³ Interestingly, in our case the Z-spectrum showed also a CEST effect at -17 ppm (Figure 1). We hypothesize that the signals at 11 and -17 ppm stem from an ensemble of nonspherical liposomes with different orientations in the magnetic field.¹⁵ Above T_m , $[\text{Tm}(\text{hpdo}3\text{a})(\text{H}_2\text{O})]$ was released from the aqueous inner compartment of the liposome as deduced from the absence of those signals in the Z-spectrum measured at 315 K, which did not reappear upon cooling to 298 K.

In Figure 2, the CEST effect at 11 ppm and the integral of the ^{19}F NMR signal (doublet, $^1J_{\text{PF}} = 709 \text{ Hz}$) are plotted as a function of temperature. As long as the shift agent remained intraliposomal ($T < 308 \text{ K}$), a high CEST effect was observed, whereas the intensity of the simultaneously measured ^{19}F NMR signal was negligible. Upon further temperature increase the CEST signal vanished and the ^{19}F signal showed a sharp increase to a thereafter constant value. The low initial ^{19}F NMR signal intensity of the encapsulated NH_4PF_6 is ascribed to spectral broadening due to the high concentration of the paramagnetic shift agent in combination with a nonspherical liposomal carrier.¹⁶ This effect is reduced upon release of the liposomal content when approaching T_m (as determined by DSC, upper panel in Figure 2), which results in sharper ^{19}F peaks (Figure S3).

Corresponding images (Figure 3) were obtained on a 3.0 T clinical MRI scanner (Achieva, Philips Healthcare, The Netherlands) equipped with a 7 cm solenoid transmit/receive coil, dual tuned to ^{19}F and ^1H resonance frequencies. With a saturation power of $3.6 \mu\text{T}$ at $\pm 12 \text{ ppm}$, the 2D CEST MR images were recorded with a single-shot fast spin echo technique within 75 s (24 averages, resolution 0.8 mm). The CEST effect was 7.3% at 295 K. A 2D gradient-echo technique was used to image NH_4PF_6 within 200 s (1.9 mm resolution), using an echo time of 3 ms to acquire the ^{19}F MR signal in phase.

In conclusion, a new concept for MR image-guided drug delivery has been presented. Our approach employs novel temperature-

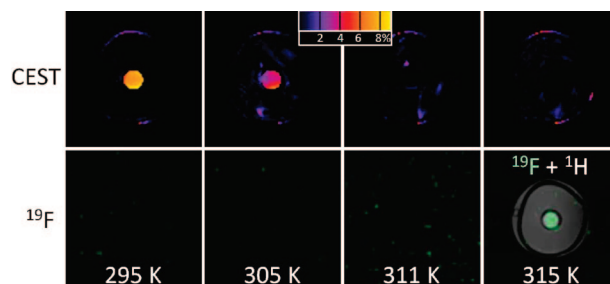


Figure 3. ^1H lipoCEST and ^{19}F MR images of temperature-sensitive liposomes on a clinical 3.0 T MRI scanner. The CEST signal (color scale in percent) vanished at $T \geq 311 \text{ K}$ while the fluorine signal appeared at 315 K (overlay with the ^1H image for colocalization and clarity).

sensitive liposomal contrast agents, which allow drug carrier localization using ^1H CEST MRI with simultaneous observation and quantification of drug release using ^{19}F MR imaging in response to a local temperature increase. This new class of temperature-sensitive imaging agents creates the opportunity to significantly improve localized therapy with liposomal drug carriers using focused ultrasound under MR image guidance.

Acknowledgment. The authors thank Danielle Beelen for the NMR studies, Dr. Marcel Verheijen for the cryo-TEM analysis, and Dr. Henk Keizer (SyMO-Chem, The Netherlands) for the synthesis of $[\text{Tm}(\text{hpdo}3\text{a})(\text{H}_2\text{O})]$. This study was funded in part by the Integrated EU Project MEDITRANS (FP6-2004-NMP-NI-4/IP 026668-2).

Supporting Information Available: Experimental details, cryo-TEM images, and the CEST effect versus the saturation frequency offset. This material is available free of charge via the Internet at <http://pubs.acs.org>.

References

- (1) Torchilin, V. P. *Nat. Rev. Drug Discovery* **2005**, *4*, 145–160.
- (2) Dromi, S.; Frenkel, V.; Luk, A.; Traugher, B.; Angstadt, M.; Bur, M.; Poff, J.; Xie, J.; Libutti, S. K.; Li, K. C. P.; Wood, B. J. *Clin. Cancer Res.* **2007**, *13*, 2722–2727.
- (3) Needham, D.; Anyarambhatla, G.; Kong, G.; Dewhirst, M. W. *Cancer Res.* **2000**, *60*, 1197–1201.
- (4) Salomir, R.; Palussière, J.; Fosshelm, S. L.; Rogstad, A.; Wiggen, U. N.; Grenier, N.; Moonen, C. T. W. *J. Magn. Reson. Imaging* **2005**, *22*, 534–540.
- (5) Ward, K. M.; Aletras, A. H.; Balaban, R. S. *J. Magn. Reson.* **2000**, *143*, 79–87.
- (6) Aime, S.; Delli Castelli, D.; Terreno, E. *Angew. Chem., Int. Ed.* **2002**, *41*, 4334–4336.
- (7) Zhang, S.; Trokowski, R.; Sherry, A. D. *J. Am. Chem. Soc.* **2003**, *125*, 15288–15289.
- (8) Zhang, S.; Malloy, C. R.; Sherry, A. D. *J. Am. Chem. Soc.* **2005**, *127*, 17572–17573.
- (9) Zhou, J.; van Zijl, P. C. M. *Prog. Nucl. Magn. Reson. Spectrosc.* **2006**, *48*, 109–136.
- (10) Pikkemaat, J. A.; Wegh, R. T.; Lamerichs, R.; van de Molengraaf, R. A.; Langereis, S.; Burdinski, D.; Raymond, A. Y. F.; Janssen, H. M.; de Waal, B. F. M.; Willard, N. P.; Meijer, E. W.; Grüll, H. *Contrast Media Mol. Imaging* **2007**, *2*, 229–239.
- (11) Aime, S.; Delli Castelli, D.; Terreno, E. *Angew. Chem., Int. Ed.* **2005**, *44*, 5513–5515.
- (12) Aime, S.; Delli Castelli, D.; Lawson, D.; Terreno, E. *J. Am. Chem. Soc.* **2007**, *129*, 2430–2431.
- (13) Terreno, E.; Cabella, C.; Carrera, C.; Delli Castelli, D.; Mazzon, R.; Rollet, S.; Stancanelli, J.; Visigalli, M.; Aime, S. *Angew. Chem., Int. Ed.* **2007**, *46*, 966–968.
- (14) $\text{H}_2\text{hpdo}3\text{a} = 10$ -(2-hydroxypropyl)-1,4,7,10-tetraazacyclododecane-1,4,7-triacetic acid.
- (15) Delli Castelli, D.; Terreno, E.; Carrera, C.; Giovenzana, G. B.; Mazzon, R.; Rollet, S.; Visigalli, M.; Aime, S. *Inorg. Chem.* **2008**, *47*, 2928–2930.
- (16) Mizukami, S.; Takikawa, R.; Sugihara, F.; Hori, Y.; Tochio, H.; Wälchli, M.; Shirakawa, M.; Kikuchi, K. *J. Am. Chem. Soc.* **2008**, *130*, 794–795.

JA8087532